DYNAMIC FRONT TRANSITIONS AND SPIRAL-VORTEX NUCLEATION

Christian Elphick[1], Aric Hagberg[2], and Ehud Meron[3]

[1] Department of Physics, Universidad Técnica Federico Santa Maria, Valparaiso, Casilla 110-V, Chile
[2] Program in Applied Mathematics, University of Arizona, Tucson, AZ 85721
[3] Department of Mathematics and ACMS, University of Arizona, Tucson, AZ 85721

(August 1994)

This is a study of front dynamics in reaction diffusion systems near Nonequilibrium Ising-Bloch bifurcations. We find that the relation between front velocity and perturbative factors, such as external fields and curvature, is typically multivalued. This unusual form allows small perturbations to induce dynamic transitions between counter-propagating fronts and nucleate spiral vortices. We use these findings to propose explanations for two experimental observations: Spiral breakup driven by convection, and spot splitting.

PACS numbers: 05.45.+b,82.20.Mj

Nonequilibrium Ising-Bloch (NIB) transitions [1] have been identified recently as important mechanisms of pattern formation in reaction-diffusion [2,3] and liquid crystal [4] systems. Mathematically, a NIB transition amounts to a pitchfork bifurcation where a stationary (Ising) front loses stability to a pair of counter-propagating (Bloch) fronts. The coexistence of two Bloch fronts far beyond the bifurcation allows the formation of regular patterns such as periodic traveling domains and rotating spiral waves.

In this Letter we show that near a NIB bifurcation spontaneous transitions between the two Bloch fronts become feasible and that a number of apparently unrelated phenomena can be understood in terms of these transitions. Front transitions of this kind can be induced by extrinsic perturbations, such as advective fields, or intrinsic perturbations, such as front interactions and curvature. They may occur uniformly along the front, reversing its direction of propagation, or locally, nucleating spiral-vortex pairs. We study the mechanism of such transitions and propose explanations for two experimental observations: Spiral breakup induced by the onset of convection in chemical reactions [5], and spot splitting [6]. We suggest that these experiments as well as the transition from labyrinthine patterns to spiral turbulence found numerically in [7] are all realizations of the same mechanism.

The key feature that underlies front transitions is a multivalued dependence of front velocity on extrinsic and intrinsic perturbations close to a NIB bifurcation. Fig. 1 shows a typical form of such a relation. The upper and lower branches correspond to the two counter-propagating Bloch fronts. At least one of them terminates at a *realizable* perturbation strength. A perturbation that drives the system to the end of a given Bloch front branch induces a transition to the other branch as indicated by the arrow.

We consider a nongradient reaction-diffusion system of the form

$$u_t = u - u^3 - v + \nabla^2 u, \qquad (1a)$$

$$v_t = \epsilon(u - a_1 v - a_0) + \mathbf{J}\cdot\nabla v + \delta\nabla^2 v, \qquad (1b)$$

where $\mathbf{J}$ represents an external vector field. In the context of chemical reactions u and v represent concentrations of two key chemical species, and $\mathbf{J}$ may stand for a convective flow field. We note that there is no apriori reason to assume that both species are advected differently by the flow field. However, chemical reactions normally involve many more than two chemical species. Two-variable models like (1) are obtained by adiabatic elimination of fast reacting species, and in this process transport terms are renormalized. As shown by Dawson *et al.* [8] this can lead to an effective differential flow as assumed in (1).

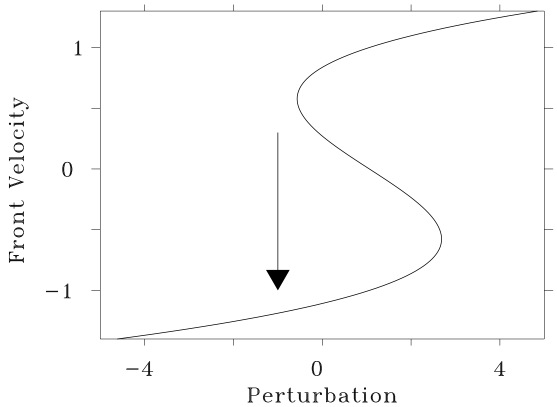

FIG. 1. A typical front-velocity vs. perturbation graph near a NIB bifurcation. The figure is a plot of V vs. I according to the stationary form of (3) with $\alpha_0 = -2.0$ and $a_1 = 5.0$.

We begin with the simpler case of a non-diffusive v field, $\delta = 0$, in one space dimension, x, and consider first the symmetric system, $a_0 = 0$, with no external field, $\mathbf{J} = 0$. We choose a_1 such that equations (1) describe a bistable medium having two linearly stable, stationary homogeneous states: An up state, (u_+, v_+), and a down state, (u_-, v_-), where $u_+ = -u_- = \sqrt{(1 - a_1^{-1})}$, and $v_+ = -v_- = a_1^{-1}u_+$. The system (1) has a stationary (Ising) front solution, $u_0(x) = -u_+\tanh(u_+x/\sqrt{2})$,

$v_0(x) = a_1^{-1}u_0(x)$, connecting the up state at $x = -\infty$ to the down state at $x = \infty$. This front solution exists for all $\epsilon > 0$. For $\epsilon < \epsilon_c = a_1^{-2}$, however, two additional (Bloch) front solutions appear, propagating at velocities $c = \pm[\frac{5}{2u_+^2}(\epsilon_c - \epsilon)]^{1/2}$. Their leading-order forms for $|c| \ll 1$ are $u(x,t) = u_0(x - ct)$ and $v(x,t) = a_1^{-1}u_0(x - ct + ca_1)$ [3]. To that order, the Bloch front structure differs from the Ising front structure in that the v field is translated with respect to the u field by an amount proportional to c.

Our first objective is to derive an order parameter equation describing dynamic transitions between the two Bloch fronts. We take the order parameter to be the time-dependent front velocity, V, normalized such that $V = 0$ corresponds to the Ising front and $V = \pm 1$ to the two Bloch fronts. The actual front velocity is given by $C = cV$. Notice that the velocity sign has been absorbed in V. We derive an evolution equation for V using asymptotic expansions in the small positive parameter c and demanding uniform validity. We write $u(z,T) = u_0(z) + \sum_{n=1}^{\infty} c^n u_n(z,T)$ and $v(z,T) = v_0(z) + \sum_{n=1}^{\infty} c^n v_n(z,T)$, where $z = x - \zeta(T)$, and $T = c^2 t$. The normalized velocity is defined as $V(T) = c\zeta_T$. We also expand $\epsilon = \sum_{n=0}^{\infty} c^n \epsilon_n$ and use these expansions in (1). Solvability conditions at orders c and c^2 yield $\epsilon_0 = \epsilon_c = a_1^{-2}$ and $\epsilon_1 = 0$, respectively. At order c^3 we obtain the order parameter equation

$$V_T = \mu V(1 - V^2), \qquad \epsilon < \epsilon_c, \tag{2}$$

where $\mu = a_1|\epsilon_2| = 2a_1u_+^2/5 > 0$. Equation (2) reproduces the Ising and the Bloch front solutions of (1) as constant speed solutions with $V = 0$ and $V = \pm 1$, respectively. It also contains information about the stability of these solutions (for $\epsilon < \epsilon_c$) with respect to Galilean boosts: The Ising front is unstable and the Bloch fronts are stable.

Next, we consider the nonsymmetric case, $a_0 \neq 0$, with constant convective perturbation $\mathbf{J} = J\hat{\mathbf{x}}$. For simplicity we take $a_0 = c^3\alpha_0$ and $J = c^3 I$, where α_0 and I are of order unity. The order parameter equation now reads

$$V_T = \mu V(1 - V^2) + \nu\alpha_0 + \frac{1}{a_1}I, \tag{3}$$

where $\nu = \frac{3}{\sqrt{2}a_1(a_1-1)}$. One immediate result that follows from (3) is a multivalued relation, of the form shown in Fig. 1, between the constant velocity of a front and the convective perturbation I (or J). Another feature of (3) is that it describes a gradient flow (despite the nongradient nature of (1)) derivable from the potential

$$\mathcal{U} = \mu\frac{V^2}{2}\Big[\frac{V^2}{2} - 1\Big] - \Big(\nu\alpha_0 + \frac{1}{a_1}I\Big)V.$$

In a range of I values, $I_{min}(a_0) < I < I_{max}(a_0)$, $\mathcal{U}(V)$ is a double well potential. The wells at $V = V_- < 0$ and $V = V_+ > 0$ pertain to Bloch fronts propagating to the left and to the right, respectively. Decreasing I below I_{min} leads to the disappearance of the well at V_+ or the Bloch front that propagates to the right. Since the dynamics are gradient, convergence to the well at $V = V_-$ follows. This amounts to a transition from a Bloch front propagating to the right (upper branch in Fig. 1) to a Bloch front propagating to the left (lower branch in Fig. 1), induced by the convective perturbation J.

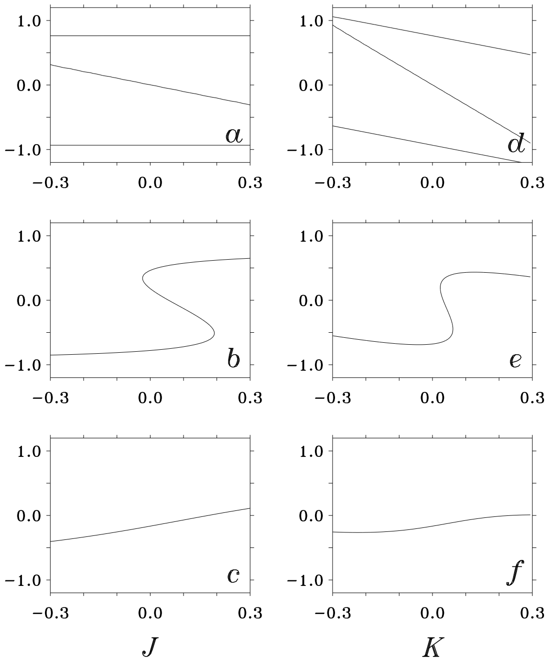

FIG. 2. Front velocity, C, vs. advective perturbation, J, and curvature, K, for $\delta/\epsilon \gg 1$: (a,d) deep in the Bloch regime, (b,e) near the NIB bifurcation, (c,f) deep in the Ising regime.

We now turn to the more general case of two diffusing species, $\delta \neq 0$. The analysis of this case is harder, but for $\delta/\epsilon \gg 1$ a singular perturbation method can be applied [9]. In ref. [3] we studied the unperturbed ($\mathbf{J} = 0$) one-dimensional form of (1) using this approach. The following relation for the velocity C_0 of a front connecting the up state at $x = -\infty$ to the down state at $x = \infty$ was found:

$$C_0 = F(C_0, \eta), \;\; F(X,Y) = \frac{3X}{\sqrt{2}q^2(X^2 + 4q^2Y^2)^{1/2}} + C_\infty, \tag{4}$$

where $\eta^2 = \epsilon\delta$, $q^2 = a_1 + 1/2$ and $C_\infty = \frac{3a_0}{\sqrt{2}q^2}$. A graph of C_0 vs. η (or C_0 vs. ϵ at constant δ) yields a NIB bifurcation diagram valid for any distance from the bifurcation point as long as $\delta/\epsilon \gg 1$. Equations (4) can be used to find a relation for the front velocity C in the presence of a perturbation J. First, we rewrite equations (1) (with $\mathbf{J} = J\hat{\mathbf{x}}$) in the form

$$u_{xx} + Cu_x + u - u^3 - v = 0, \tag{5a}$$

$$\delta_J v_{xx} + Cv_x + \epsilon_J(u - a_1 v - a_0) = 0, \tag{5b}$$

where $\epsilon_J = \epsilon\Delta_J$, $\delta_J = \delta\Delta_J$ and $\Delta_J = \frac{C}{C+J}$. According to (5), front solutions of (1), the perturbed system with parameters ϵ and δ, are equivalent to front solutions of an unperturbed system with effective parameters ϵ_J and

δ_J. Using relation (4) with C_0, ϵ, and δ replaced by C, ϵ_J, and δ_J, respectively, we find

$$C = F(C + J, \eta), \tag{6}$$

where F is given by (4). Figs. $2a - 2c$ show graphs of C vs. J, obtained by solving (6) for C deep in the Bloch regime ($2a$), near the NIB bifurcation ($2b$), and deep in the Ising regime ($2c$). The multivalued form of the graph in $2b$ resembles that of the V vs. I graph obtained from (3) for $\delta = 0$.

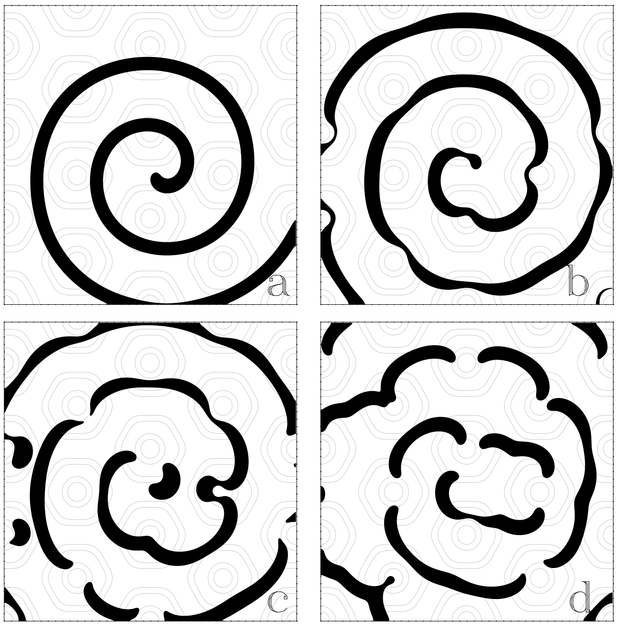

FIG. 3. Breakup of a spiral wave induced by a hexagonal convective pattern. The light and dark regions correspond to down and up states, respectively. The dotted curves denote contours of constant convection speed. The convection flow direction is outward from the centers of the hexagons. Frame a is the unperturbed spiral wave and frames b, c, d are taken at times $t = 100,\ 140,\ 220$ from the onset of the convective pattern. Parameters used: $a_0 = -0.1$, $a_1 = 2.0$, $\epsilon = 0.032$, $\delta = 0.9$, $A = 1.59$ and $Q = 0.06283$.

We now relate our results to experimental observations of convection induced disorder in the Belousov-Zhabotinsky (BZ) reaction [5]. In these experiments convection in the form of Bénard cells was induced by evaporative cooling of the free surface of the BZ solution. The onset of convection initiated processes of spiral breakup and spiral wave nucleation which destroyed the order of the pre-existing chemical pattern.

Consider a stripe of an up-state domain propagating through a two-dimensional hexagonal convective pattern (see Fig. 4). The leading and trailing fronts of the stripe correspond to the upper and lower branches in Fig. 1 (or $2b$), respectively. Assume that the reaction parameters are tuned so that the point of zero perturbation, $J = 0$, on the upper branch in Fig. 1 lies close to the left end of this branch. In other words, the leading front is only weakly stable to a front transition. As the stripe propagates through the hexagonal convective pattern, alternating portions of its leading front experience phases during which $J = \mathbf{J} \cdot \hat{\mathbf{n}} < 0$, i.e. the convective field has a component pointing in a direction opposite to the direction of propagation, $\hat{\mathbf{n}}$. If the convective field is strong enough, local front transitions may take place, driving portions of the leading front from the upper branch past the end point to the lower branch. These transitions nucleate a spiral-vortex pair for each Bénard cell the stripe crosses. Portions of the leading front that undergo front transitions eventually annihilate with the trailing front, breaking the stripe into disjoint pieces. Note that the trailing front does not undergo front transitions because of its higher stability.

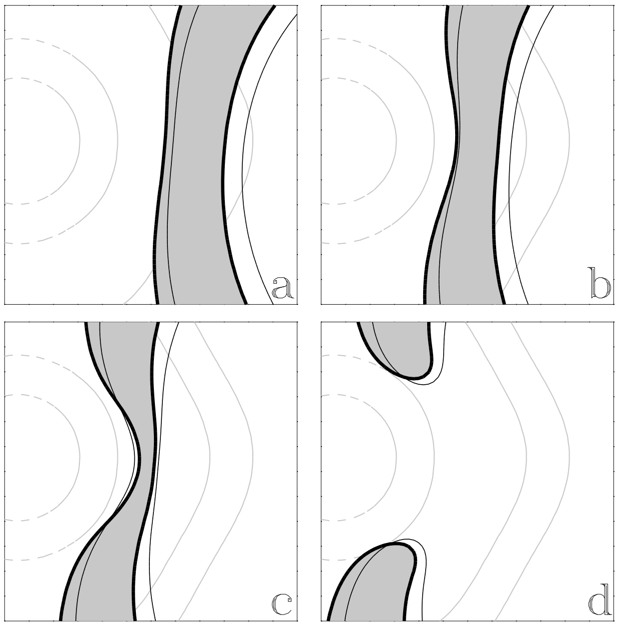

FIG. 4. A closer look at a typical breakup process in Fig. 3. The thick (thin) lines are contours of $u = 0$ ($v = 0$). The direction of front propagation follows from the rule that the $v = 0$ contour always lags behind the $u = 0$ contour. The frames a, b, c, d pertain to times $t = 140,\ 160,\ 180,\ 200$. They show a local front transition, accompanied by the nucleation of a vortex pair (the crossing points of the contour lines), and the breakup of the up state domain. Parameters are the same as in Fig. 3.

Figs. 3 and 4 show numerical simulations that demonstrate these effects. We integrated (1) with Neumann boundary conditions and $\mathbf{J} = \nabla\phi$ where $\phi = A\sum_{i=1}^{3}\cos(\mathbf{q}_i \cdot \mathbf{x})$ with $\mathbf{q}_1 = (Q, 0)$, $\mathbf{q}_2 = (-Q/2, \sqrt{3}Q/2)$, $\mathbf{q}_3 = (-Q/2, -\sqrt{3}Q/2)$. Fig. 3 shows the breakup of a spiral wave once a convective field is switched on. Fig. 4 shows a closer look at the processes involved. We note that the actual experimental situation is more complex since the system is three dimensional and the flow at the bottom is in the opposite direction to the flow at the top.

So far we have studied the effects of an extrinsic perturbation. We focused on convection, but other perturbations inducing differential advection, like an electric field [10], may give rise to a similar phenomenology. Even without extrinsic perturbations there exist intrinsic factors, such as curvature and front interactions, that affect planar front propagation. We now address the effect of curvature near a NIB bifurcation. In ref. [7] we have found the following relation between the normal velocity of a front, C, and its curvature, K:

$$C = F(C + \delta K, \eta) - K, \tag{7}$$

where F is given by (4). Graphs of C vs. K deep in the Bloch regime, near a NIB bifurcation, and deep in the Ising regime, are shown in Figs. $2d$, $2e$ and $2f$, respectively. A comparison of these figures with Figs. $2a$-$2c$ indicates that the multivalued dependence depicted in Fig. 1 is a general feature of front dynamics near a NIB bifurcation. Perturbations of different nature, curvature and an advective field in this case, can have the same effect of inducing front transitions.

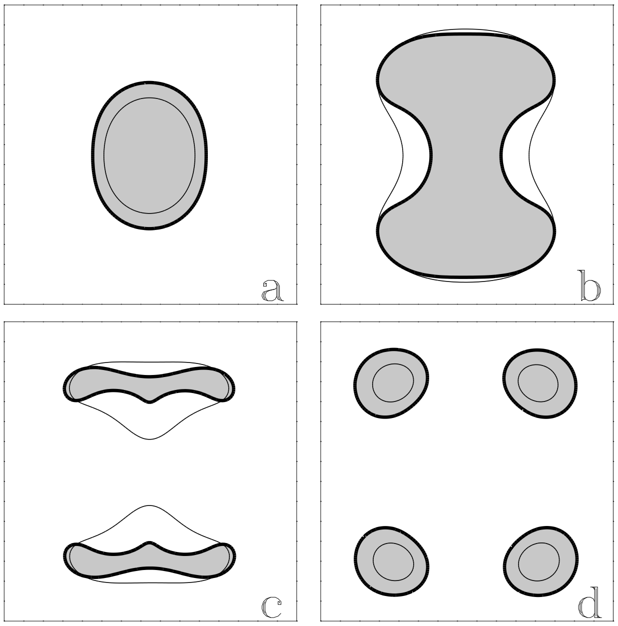

FIG. 5. Spot splitting induced by curvature variations. The frames a, b, c, d pertain to times $t = 80,\ 240,\ 280,\ 340$. Local front transitions occur at the flatter portions of the expanding front. They are accompanied by nucleation of vortex pairs, and followed by spot splitting. Parameters used: $a_0 = -0.15$, $a_1 = 2.0$, $\epsilon = 0.014$, $\delta = 3.5$.

Recently, an intriguing pattern formation phenomenon has been observed in numerical and laboratory experiments [6,11]. An expanding chemical spot was found to lose its circular shape and split into two spots. Newborn spots followed the same course of events, filling eventually the reaction domain. We suggest that spot splitting can result from dynamic front transitions induced by curvature variations. Imagine a C vs. K relation in which the upper branch terminates at a small *positive* curvature value, as depicted in Fig. $2e$. The leading front of an expanding disk-like domain corresponds to the upper branch. As the domain expands the front curvature decreases. When it falls below the critical curvature pertaining to the edge of the upper branch, a front transition occurs. As a result the domain stops expanding and begins shrinking. We have verified this scenario numerically using a circularly symmetric version of (1) (with $\mathbf{J} = 0$). Two-dimensional realizations of disk-like domains are never perfect; there are always flatter parts of the front which undergo the transition first. This leads to vortex nucleation and spot splitting as shown in Fig. 5 for an initially oval-shaped domain.

The transition from labyrinthine patterns to spiral turbulence found in [7] follows from a similar velocity-curvature relation except that the upper branch terminates near zero or at negative curvature values. In that case the mechanism that drives the leading front past the end point is the transverse instability which produces segments with negative curvature.

We have studied a particular reaction diffusion model but we believe the results are also applicable to other systems undergoing a NIB bifurcation. It would be interesting to test the ideas presented here on the liquid crystal system studied by Frisch *et al.* [4].

We thank Kyoung Lee, John Pearson, Harry Swinney and Art Winfree for interesting discussions. This work was supported in part by the Arizona Center for Mathematical Sciences (ACMS), sponsored by AFOSR. One of us (A.H.) acknowledges the support of the Computational Science Graduate Fellowship Program of the Office of Scientific Computing in the Department of Energy.

[1] P. Coullet, J. Lega, B. Houchmanzadeh, and J. Lajzerowicz, Phys. Rev. Lett. **65**, 1352 (1990).
[2] A. Hagberg and E. Meron, Phys. Rev. E **48**, 705 (1993).
[3] A. Hagberg and E. Meron, Nonlinearity **7**, 805 (1994)
[4] T. Frisch, S. Rica, P. Coullet, and J.M. Gilli, Phys. Rev. Lett. **72**, 1471 (1994).
[5] K.I. Agladze, V.I. Krinsky and A.M. Pertsov, Nature **308**, 834 (1984); S.C. Müller, T. Plesser and B. Hess, in *Physicochemical Hydrodynamics: Interfacial Phenomena*, Ed. M.G. Velarde (Plenum Press, New York, 1988).
[6] K.J. Lee, W.D. McCormick, H.L. Swinney, and J.E. Pearson, Nature **369**, 215 (1994).
[7] A. Hagberg and E. Meron, Phys. Rev. Lett. **72**, 2494 (1994).
[8] S.P. Dawson, A. Lawniczak, and R. Kapral, J. Chem. Phys. **100**, 5211 (1994).
[9] H. Ikeda, M. Mimura, and Y. Nishiura, Nonl. Anal. TMA **13**, 507 (1989).
[10] S. Schmidt and P. Ortoleva, J. Chem. Phys. **67**, 3771 (1977); O. Steinbock, J. Schütze, ans S.C. Müller, Phys. Rev. Lett. **68**, 248 (1992). **72**, 2494 (1994).
[11] J.E. Pearson, Science **261**, 189 (1993).